Eur. Phys. J. AP **6**, 95–100 (1999)

THE EUROPEAN PHYSICAL JOURNAL APPLIED PHYSICS

Stability region studies of CO_2 gas laser mixture RF capacitative discharges

S.M.A. Durrani[1,a], P. Vidaud, and D.R. Hall[2]

[1] Laser Research Laboratory, Center for Applied Physical Sciences, Research Institute, King Fahd University of Petroleum and Minerals, Dhahran 31261, Saudi Arabia

[2] Optoelectronics and Laser Engineering, Heriot-Watt University, Edinburgh EH14 4AS, UK

Received: 4 September 1998 / Revised and Accepted: 5 January 1999

Abstract. Results on the stability regions of alpha (α) to gamma (γ) transition for CO_2 gas laser mixture 3He:1CO_2:1N_2 RF capacitative discharges with and without the addition of Xe are presented in terms of current, voltage and power characteristics. Measurements have also been made of the mean electron energy, neutral gas temperature and time averaged visible emission for different electrode separations, frequencies and intermediate pressures. It is found that the Xe addition has increased the neutral gas temperature and transition input power, while it has decreased the mean electron energy and transition voltage. The time averaged visible emission has shown strong CO and NO emission from the discharge.

PACS. 52.80.-s Electric discharges – 52.80.Pi High-frequency discharges – 52.80.Tn Other gas discharges

1 Introduction

RF capacitative discharges are being increasingly used in CO_2 lasers because of a number of advantages that they have on the DC discharges [1–3]. These advantages includes low inter-electrode voltages, improved discharge stability and higher efficiencies [4]. RF discharges at intermediate pressures can occur in two distinct stable regimes, namely α and γ types [5–7]. The lower power density α-type discharge is characterized by having poorly conducting and positively charged sheaths at the electrodes boundaries and relatively low current densities, and by being sustained mainly by volume ionization. These space-charged sheaths along the boundaries of the plasma determine to a considerable degree the properties of RF discharges, since a significant portion of the interelectrode voltage is dropped across them and they can provide extra ionization for the volume of the discharge. Sheaths also play an important role in the transition from α to γ RF discharges [5–7]. If the power to an α discharge is raised to a critical value, which depends on the gas and the other discharge parameters, a transition occur to the γ-type discharge. The γ-type discharge has certain similarities to the DC glow: it tolerates high power densities, is sustained by wall ionization processes and has relatively thin electrode boundary sheaths and high displacement and conduction current. RF discharges at intermediate pressures, however cannot yet be fully exploited because at presence they are not well-understood [8,9].

In spite of the rapid development of RF lasers [3,4,10,11] very little has been published on the experimentally observable properties of the discharge itself such as voltage and current characteristics and spectroscopy of the visible and IR emission [8]. Three areas are of particular interest; namely the mapping of the parameter space which allow stable α discharges used for the CO_2 laser excitation secondly the development of an understanding of the inhomogeneities or striations [12,13] and thirdly the plasma processes giving rise or *vice versa* to the laser performance so important in these transverse excited discharges considered here where the interelectrode separation is small. In this paper experimental results are presented on the characteristics of the α discharges and arc like γ-type discharge which results when the power loading of the α discharge exceeds a critical value. The transition from the α to γ type RF discharge is important in devices such as CO_2 and CO lasers as it places an upper limit on the power density that the α discharge used can accommodate. Experiments are of the laser mixture 3He:1CO_2:1N_2, with and without the addition of xenon.

2 Experimental

For all the experiments reported in this paper, we used the same static gas RF discharge chamber and techniques described in detailed elsewhere [7,9,14–16]. In brief, the aluminum electrodes were Bruce-profiled discs of diameter 2.8 cm that were independently water cooled and could be moved to a separation of up to 2.0 cm. The

[a] e-mail: smayub@kfupm.edu.sa

discharge power was supplied by an oscillator deriving a wide-band ENI 5100L power amplifier fed through a Bird Thruline 4431 watt meter and an external discharge impedance matching circuit. For the experimental work presented here the discharge impedance was matched perfectly for the CO_2 gas laser mixture with and without the addition of xenon, and the reflected power was always kept below 3%. The gases (3He:1CO_2:1N_2) were research grade, and the metal vacuum chamber could be evacuated to 10^{-3} torr. The interelectrode voltage was measured using a capacitative divider, and oscilloscope or electronic voltmeter. The discharge current was obtained by measuring the voltage across a $\sim 1.0\ \Omega$ thick carbon film resistor R placed between the bottom electrode and earth. For the measurements with Au surfaces, Au was evaporated directly onto the Al electrodes. The electron temperatures were measured using floating double electrostatic probe technique [14–16]. The neutral gas temperature was measured with an Hg thermometer placed outside the discharge field zone and 2 cm from the luminous edge of the discharge. Visible emission from the discharge was detected with an array of five optical fibers that could be tracked in three dimensions. The spectroscopic measurements were taken using Spex monochromator with line calibration provided by a mercury-cadmium lamp. The equipment for the voltage, current and light measurements was contained in an RF shielded cage. The errors in measuring gas pressure, voltage, current, power, frequency, interelectrode separation, discharge cross-sectional area, neutral gas temperature and mean electron energy are estimated at respectively 5%, 10%, 10%, 5%, 1%, 2%, 20%, 10% and 20%.

3 Results and discussion

3.1 Current, voltage and power characteristics

The current, voltage and power characteristics of α and γ type RF capacitative discharge in the CO_2 gas laser mixture (3He:1CO_2:1N_2) have the general features as those of N_2 [7], illustrated in Figures 1 and 2. As the voltage is increased from $V_{\alpha_{\min}}$ (minimum α maintenance voltage) the current increases fairly linearly to the $V_{\alpha_{\max}}$ point where an abrupt α to γ change occurs and the voltage falls to the $V_{\gamma \mathrm{tr}}$ points. The dotted line shows the forward transition path. Further increase in input power from the $V_{\gamma \mathrm{tr}}$ results in a further, but much more gradual decrease in the RF voltage, as illustrated by the arrow pointing in the forward path of the input power. For discharges in the CO_2 gas laser mixture (3He:1CO_2:1N_2) it was found that the backward transition of γ to α is possible. It was also observed that after the reverse transitions (γ to α), the RF voltage was larger for the same input power at $V_{\alpha_{\min}}$ point. In comparison to the results with N_2 [7], there is considerable hysterises in the power, current and voltage characteristics.

The functional dependence of the α to γ transition in 3He:1CO_2:1N_2 mixture again has the similar features

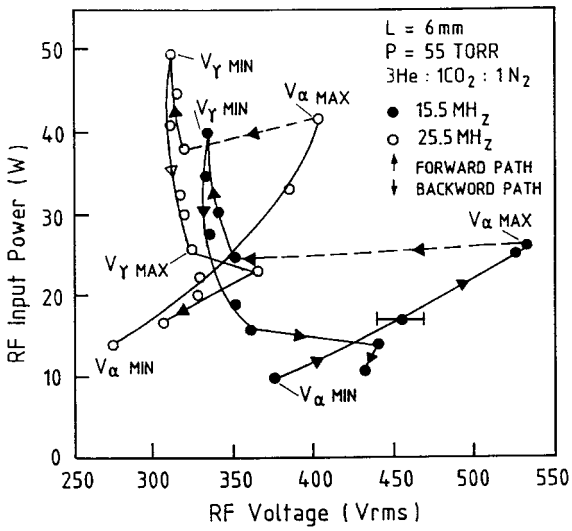

Fig. 1. 3He:1CO_2:1N_2, α and γ total discharge power and voltage characteristic for different RF frequencies at constant pressure and electrode separation.

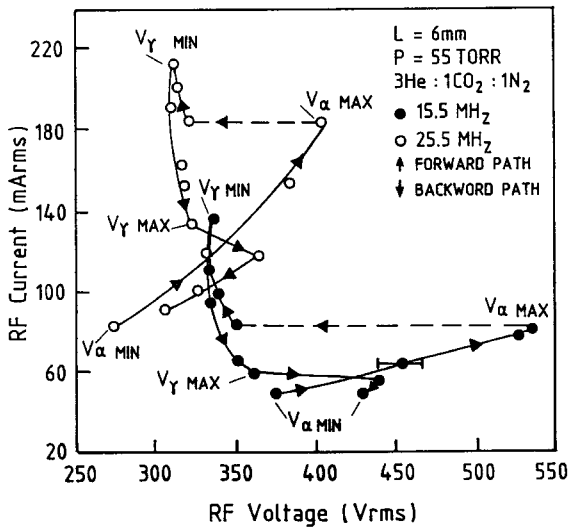

Fig. 2. 3He:1CO_2:1N_2, α and γ total discharge current and voltage characteristic for different RF frequencies at constant pressure and electrode separation.

of those in N_2 [7]. Figure 3 shows that for the similar discharge conditions of 35 torr, 15.5 MHz and 6 mm, pressure, RF frequency and electrode separation, the RF transition voltage is increased significantly for the 3He:1CO_2:1N_2 α discharge as compared to the N_2 α discharge. The transition power density for the above conditions was 1.9 W/cm^2 for N_2, and 3.0 W/cm^2 for 3He:1CO_2:1N_2 discharges. Figure 4 [7], shows the electrical equivalent circuit for α RF capacitative discharges consists of a condenser of time dependent capacitance C representing the sheath zone in contact with the instantaneous cathode and a series constant resistance R representing the rest of the discharge or plasma zone over a half cycle. It is known that the α to γ transition occurs more readily the greater the sheath mean reduced field V_s/aP, where V_s is the sheath

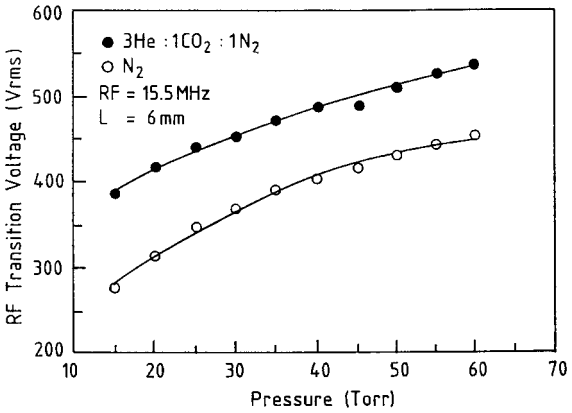

Fig. 3. α to γ transition voltage as a function of pressure for different gases at constant RF frequency and electrode separation.

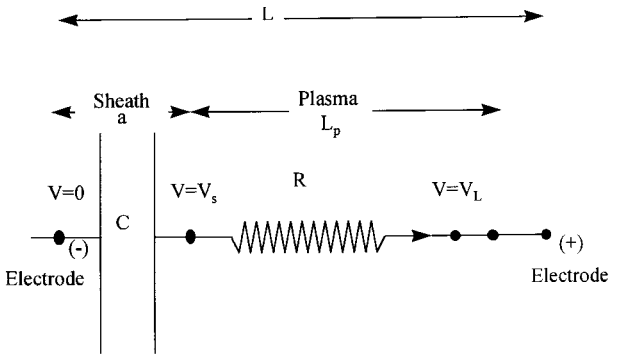

Fig. 4. An electrical equivalent circuit for α type RF discharge. L_p, L, C, R, a, V_s and V_L are the plasma zone length, inter-electrode separation, sheath capacitance, the plasma zone resistance, the electron oscillation amplitude, sheath voltage and plasma voltage respectively [7].

voltage, P is the gas pressure and a is the electron oscillation amplitude and sheath thickness, thicker the sheaths, higher would be the voltage drop across [7,15]. Figure 5 shows oscillogram traces of the visible emission profile in transverse direction of the discharge for the two gas mixtures. The sheaths are thinner in $3He{:}1CO_2{:}1N_2$ comparing with N_2 for otherwise similar discharge conditions. Thus more power is required for $3He{:}1CO_2{:}1N_2$ α to γ transitions in comparison with N_2 for the same discharge conditions. The addition of Xe to the $3He{:}1CO_2{:}1N_2$ mixture decreases the RF transition voltages as shown by Figure 6. The change in transition voltage due to the Xe addition was smaller the lower the pressure but for the higher pressures, the drop in the transition voltage was significant. Figure 7 shows that although the Xe addition reduces the RF transition voltage, the transition power is raised and the α discharge is more stable with the addition of Xe to the $3He{:}1CO_2{:}1N_2$ mixture.

The α to γ transition voltage and power is increased significantly with gold coated aluminum electrodes for otherwise the same discharge conditions as aluminum electrodes. It is generally agreed [17] that the α to γ transition is mainly controlled by secondary electron emission

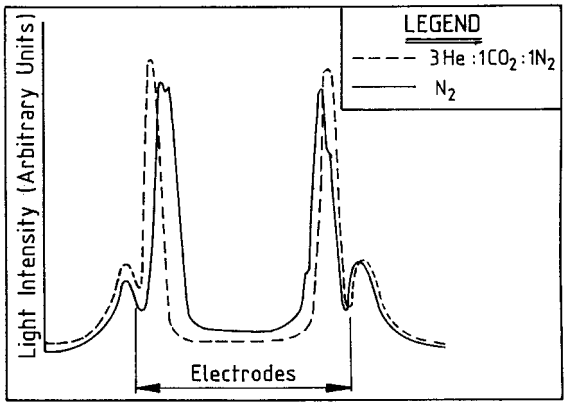

Fig. 5. Oscillogram traces of the visible emission profile from the discharge across the electrodes showing the sheath thickness for different gases at constant pressure, frequency, electrode separation, and input power of 40 torr, 40 MHz, 10 mm, and 25 W respectively.

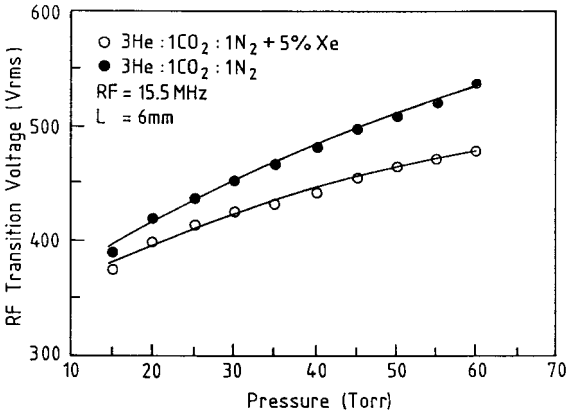

Fig. 6. α to γ transition voltage as a function of pressure for different gas mixtures at constant RF frequency and electrode separation.

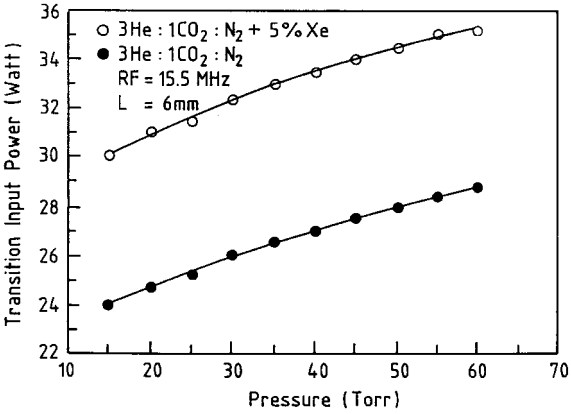

Fig. 7. α to γ transition power as a function of pressure for different gas mixtures at constant RF frequency and electrode separation.

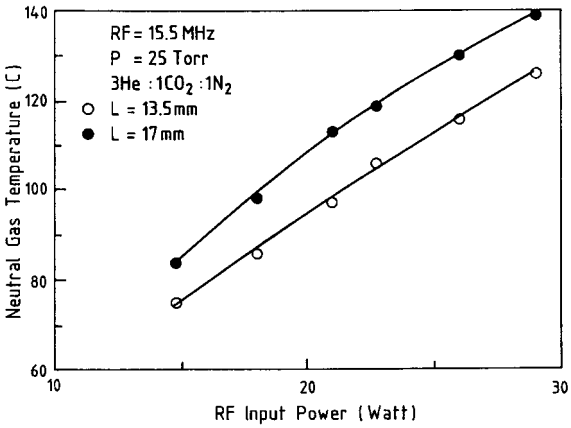

Fig. 8. 3He:1CO_2:1N_2 neutral gas temperature as a function of discharge input power for different electrode separations at constant RF frequency and pressure.

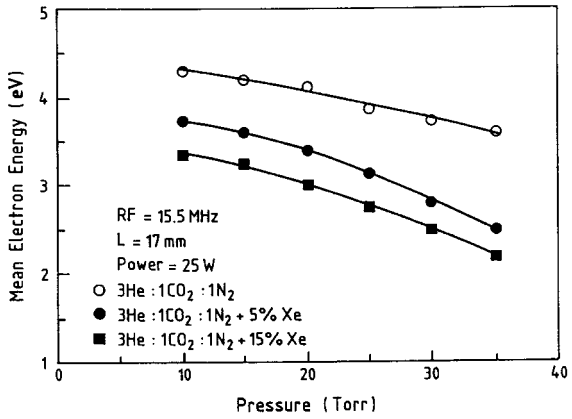

Fig. 9. Mean electron energy as a function of pressure for different gas mixtures at constant RF frequency, input power and electrode separation.

from the instantaneous cathode, therefore the observed dependence of transition voltage on electrode surface material can be explained in terms of the work functions of the materials. The lower the work function the more the secondary emission. For the two material used, gold and aluminum, gold has the higher work function.

3.2 Electron and neutral gas temperature measurements

The knowledge of electron and neutral gas temperatures permits the calculation of the plasma gain zone reduced fields (E/N) in the positive column of the α type RF discharge, which is significant in the assessment of the CO_2 laser gain medium. The increase in neutral gas temperature versus input power and electrode separation is shown in Figure 8. The increase in neutral gas temperature with electrode separation is due to the fact that the discharge is cooled by the diffusion of molecules to the water cooled electrodes and this is less effective the further apart they are. Predictably the effect of stopping the water cooling of the electrodes was to raise the discharge gas temperature. For constant power loading and different pressures no change in the gas temperature was detectable. This was due to the fact that to first approximation, the thermal conductivity of a gas does not change with pressures in the range 1–150 torr [18]. Variation with pressure of mean electron energies is shown in Figure 9, these observed mean electron energies are in the range 4.25 to 2.5 eV for the pressures of 10–35 torr respectively. The decrease in mean electron energies with pressure being due to the fact that at constant input power the plasma zone reduced field (E/N) from which electron gain energy decreases with pressure [7,16].

3.3 The effect of xenon addition on the electron and neutral gas temperatures

It is well-known that the addition of xenon to the CO_2 gas laser mixture commonly used in DC and RF excited

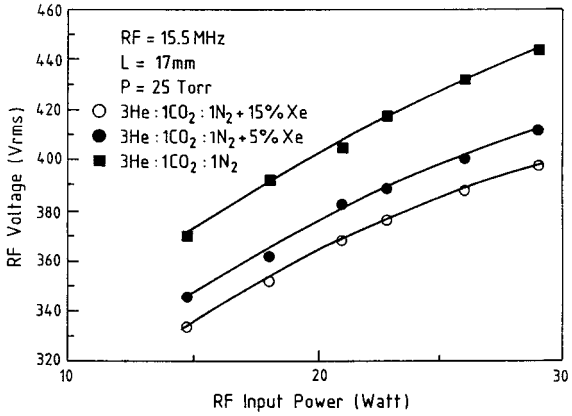

Fig. 10. α discharge RF voltage as a function of input power for different gas mixtures at constant RF frequency, pressure and electrode separation.

lasers can produce significant improvement both in laser output power and efficiency, and can also lead to an extension of sealed off life time [19–22]. The origin of these effects is attributed to the low ionization potential of xenon and its large momentum transfer collision cross-section [23]. We have repeated some of the above experiments and have extended them in an effort to clarify further the xenon influence on CO_2 gas laser. Figure 9 shows the variation in mean electron energies with total gas pressure for 3He:1CO_2:1N_2 with and without added xenon at a fixed input power, RF frequency and electrode separation of 26 W, 15.5 MHz and 17 mm respectively. It is clearly shown that when xenon is added to the 3He:1CO_2:1N_2 discharge, it has reduced the mean electron energies. Figure 10 shows the variation in RF voltage, with total input power for various amounts of added xenon at a fixed pressure, RF frequency and electrode separation. It is seen that increasing the xenon content decreases the RF voltage. Although, as shown by Figure 11 increasing the xenon content increases the neutral gas temperature and therefore decreases N, the net effect appears to be to reduce E/N and hence the electron energy as the electron

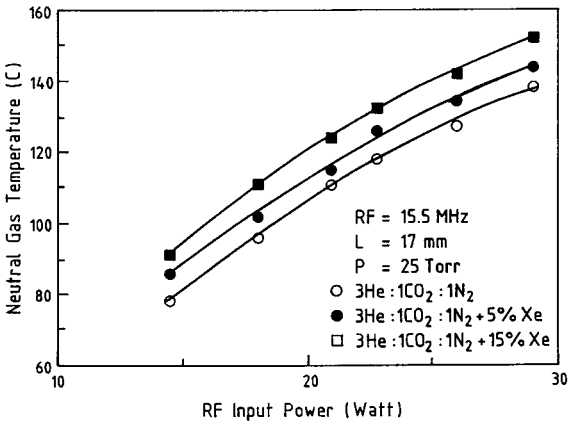

Fig. 11. Neutral gas temperature as a function of input power for different gas mixtures at constant RF frequency, pressure and electrode separation.

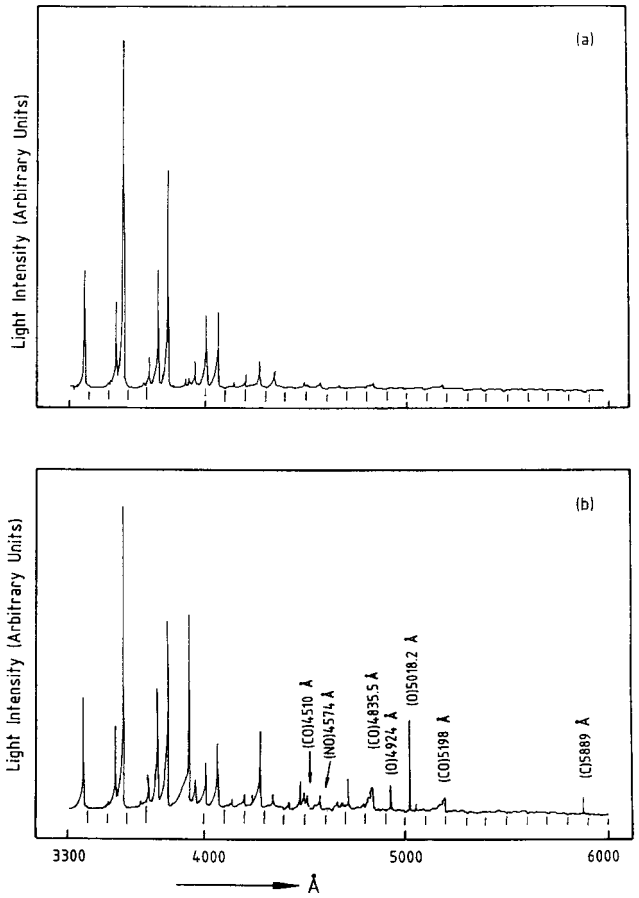

Fig. 12. The 3He:1CO_2:1N_2 emission spectra (a) α discharge and (b) γ discharge.

temperature measurements discussed above show. If this assumption is true, then the question arises, why does the output power and efficiency of the CO_2 gas laser [22] not increase when the addition of xenon to the laser mixture is increased above 5%. The answer to this question is probably that with greater percentage of xenon, not only is the gas temperature rising but the amount of CO_2 available for excitation is decreasing. The increase in neutral gas temperature with xenon is due to the decreasing percentage of helium in the mixture. Helium is included in CO_2 gas laser mixture because of its high thermal conductivity of 352×10^{-6} cal cm^{-1} s^{-1} C^{-1} [24]. The thermal conductivity of xenon is 12×10^{-6} cal cm^{-1} s^{-1} C^{-1}, which is 25 times less than helium (due to its atomic weight). Thus the presence of xenon in CO_2 laser gas mixtures on the one hand will be beneficial in decreasing the mean electron energies, but on the other hand, due to its lower thermal conductivity it will increase the neutral gas temperature, which ultimately will degrade the laser performance [25].

3.4 Spectroscopy of the time averaged visible emission

The presence of CO in CO_2 lasers is extremely important as an indicator of disassociation, particularly in sealed off CO_2, lasers, where up to 80% of the CO_2 can be disassociated [26]. Assuming that we have a reasonable density of CO present, then the cross-section for electron input pumping of CO is similar to that for N_2 except that it has a lower threshold and a higher peak. A sizable fraction of up to 15% of the electron kinetic energy can go directly into the pumping of the vibrational levels of CO [27]. The presence of NO and CO also play an important role in deexcitation of CO_2 molecule [28]. It is therefore of interest to monitor, if possible, the CO and NO emissions from the discharge.

Time averaged emission of an α and γ discharge in 3He:1CO_2:1N_2 helium 3300 Å and 6000 Å and at a resolution of about 1 Å emitted from the middle of the discharge is shown in Figures 12a and 12b. In the range 3300 Å to 4400 Å, the spectra for the two discharge types are the same as for pure N_2 [7]. Above 4000 Å the CO_2 spectrum shows considerable differences. The γ spectrum, Figure 12b shows strong CO emission due to the CO ($B^1\Sigma...A^1\Pi$) system (4510.9, 4835 and 5198 Å) and NO ($B^2\Pi...X^2\Pi$) system 4574 Å, also found are a few atomic O (5018.2, 4924 Å) and C (5889 Å) lines. The comparison of Figure 12a with Figure 12b shows the presence of all the γ discharge CO and NO lines in the α spectrum but at slightly weaker intensities the relatively strong emission of CO, NO, O and C in the γ discharge is probably due to higher charge density in γ discharge as compared to the α discharge [29].

4 Conclusions

While the general behavior of the CO_2 laser mixture discharge is similar to that of N_2 [7], there are several points of interest to be noted. The transition α and γ is reversible the reduction of the electron energy affected by the addition of Xe is confirmed by both direct measurement and voltage measurements. Again addition of Xe raises the power loading at which the α to γ transition occurs but also increases the gas temperature. The effect of Xe on neutral gas temperature will reduce its beneficial effect in

lowering the electron energies. It has also been shown that the relative degree of dissociation in the discharges could be obtained by monitoring the CO emission and that the dissociation is higher in the γ discharge than it is in the α. The gold coated electrodes has increased the stability regions of an α discharge, while on the other hand a reduction in the dissociation of CO_2 in discharges where the electrodes are covered with gold and an improvement in power output has also been found [30].

For the design of CO_2 lasers, the deductions to be made from these results concern discharge stability at high power loading and discharge gas temperature. High frequency, high gas pressure and the addition of xenon allows higher power loading. Higher frequency because of its effect on the sheath capacitance [7], makes for higher currents and charge densities.

The authors wish to express their grateful appreciation to Dr. H.J. Baker, Dr. P.E. Jackson and Dr. G.N. Pearson and I.A. Bakhtiari for helpful discussions. Dr. S.M.A. Durrani would also like to thank the King Fahd University of petroleum and Minerals Research Institute.

References

1. P.P. Chenausky, R.A. Hart, L.A. Newman, N. Hoffman, in *Proceedings of the Conference on Lasers and Elect. Optics*, Phoenix, Arizona, USA, 1982, p. 88.
2. H. Hugel, W. Schock, in *Proceedings of the Conference on Lasers and Elect. Optics*, Phoenix, Arizona, USA, 1982, p. 90.
3. D. He, D.R. Hall, Appl. Phys. Lett. **43**, 726 (1983).
4. P. Vidaud, D. He, D.R. Hall, Opt. Commun. **56**, 185 (1983).
5. S.M. Levitskii, Sov. Phys. Tech. Phys. **2**, 887 (1958).
6. V.A. Godyak, A.S. Khanneh, IEEE Plasma Sci. **14**, 112 (1986).
7. P. Vidaud, S.M.A. Durrani, D.R. Hall, J. Phys. D **21**, 57 (1988).
8. C.G. Parazolli, K.R. Chien, IEEE J. Quant. Elect. **QE22**, 479 (1986).
9. S.M.A Durrani, P. Vidaud, D.R. Hall, J. Plasma Phys. **58**, 193 (1997).
10. J.G. Xin, D.R. Hall, Opt. Commun. **58**, 420 (1986).
11. P. Vidaud, S.M.A. Durrani, D.R. Hall, Paper THT4, CLEO (Ana. California, USA , 1988).
12. A.J. Hatch, L.E. Henkroth, J. Appl. Phys. **41**, 1701 (1971).
13. D. He, C.J. Baker, D.R. Hall, J. Appl. Phys. **55**, 4120 (1984).
14. P. Vidaud, D.R. Hall, J. Appl. Phys. **57**, 1757 (1985).
15. S.M.A. Durrani, Ph.D thesis, Heriot-Watt University, UK, 1988.
16. A.H. von Engel, *Ionized Gases* (Oxford: OUP, 1965).
17. N.A. Yatsenko, Sov. Phys. Tech. Phys. **26**, 678 (1981).
18. M.N. Saha, B.N. Srivastava, *A Treatise on Heat* (The Indian Press Private Limited, Allahabad and Calcutta, 1958).
19. P.O. Clark, J.Y. Wada, IEEE J. Quant. Elect. **QE4**, 263 (1968).
20. K.J. Siemsen, Appl. Optics **19**, 818 (1980).
21. D. Souilahac, A. Gundjian, Appl. Optics **20**, 3097 (1981).
22. D. He, D.R. Hall, J. Appl. Phys. **56**, 856 (1984).
23. B.R. Brode, Rev. Mod. Phys. **5**, 257 (1983).
24. *Handbook of Chemistry and Physics* (Weast 64th Addition, CRC Press, 1984).
25. L. Taylor, Raymond, Bitterman, Rev. Mod. Phys. **41**, 26 (1969).
26. B.E. Cherrington, *Gaseous Electronics and Gas Lasers* (Pergamon Press, 1980).
27. W.L. Nighan, Appl. Phys. Lett. **15**, 355 (1969).
28. F. Al-Adel *et al.*, Chem. Phys. **74**, 413 (1983).
29. V.A. Godyak, A.S. Khanneh, IEEE Plasma Sci. **PS14**, 112 (1986).
30. J. Macken, H. Wrends, M. Samis, Paper FD3, CLEO (Ana., California, USA, 1988).